Biochemical and Biophysical Research Communications 391 (2010) 651–658

Contents lists available at ScienceDirect

Biochemical and Biophysical Research Communications

journal homepage: www.elsevier.com/locate/ybbrc

NSA2, a novel nucleolus protein regulates cell proliferation and cell cycle

Heyu Zhang [a,b,1], Xi Ma [a,b,d,1], Taiping Shi [c], Quansheng Song [a,b], Hongshan Zhao [a,b,*], Dalong Ma [a,b]

[a] Department of Immunology, School of Basic Medical Sciences, Peking University, No. 38 Xueyuan Road, Beijing 100191, PR China
[b] Human Disease Genomics Center, Peking University, No. 38 Xueyuan Road, Beijing 100191, PR China
[c] Chinese National Human Genome Center, Beijing. #3-707 North YongChang Road BDA, Beijing 100176, PR China
[d] State Key Lab of Animal Nutrition, China Agricultural University, No. 2 Yuanmingyuan West Road, Beijing 100193, PR China

ARTICLE INFO

Article history:
Received 13 November 2009
Available online 22 November 2009

Keywords:
NSA2
Nuclear localization signals
Cell proliferation
Cell cycle

ABSTRACT

NSA2 (Nop seven-associated 2) was previously identified in a high throughput screen of novel human genes associated with cell proliferation, and the NSA2 protein is evolutionarily conserved across different species. In this study, we revealed that NSA2 is broadly expressed in human tissues and cultured cell lines, and located in the nucleolus of the cell. Both of the putative nuclear localization signals (NLSs) of NSA2, also overlapped with nucleolar localization signals (NoLSs), are capable of directing nucleolar accumulation. Moreover, over-expression of the NSA2 protein promoted cell growth in different cell lines and regulated the G1/S transition in the cell cycle. SiRNA silencing of the *NSA2* transcript attenuated the cell growth and dramatically blocked the cell cycle in G1/S transition. Our results demonstrated that NSA2 is a nucleolar protein involved in cell proliferation and cell cycle regulation.

Introduction

NSA2 (Nop seven-associated 2), also known as *TINP1* (TGF-β inducible nuclear protein 1) and Hairy cell leukemia protein 1 (*HCL-G1*), was originally identified as one of the putative tumor suppressor genes involved in the pathogenesis of HCL [1]. *NSA2* mRNA could be up-regulated by stimulation with TGF-β (J.S. Zhang and D.I. Smith, as annotated in the NCBI database). It was also identified in a search of *Saccharomyces cerevisiae* ORFs in yeast EST databases homologous to mammalian genes, followed by screening of a human skeletal muscle cDNA library [2]. NSA2 was found in the nucleoli of HeLa cells using mass-spectrometry [3,4], and its yeast homolog Nsa2 is an unstable pre-60S factor required for the processing of the 27 SB pre-rRNAs. The absence of Nsa2 leads to defective ribosome biogenesis, which can be complemented by human NSA2 [5]. The Nsa2 homolog in *Bombyx mori* (BmTINP1) is thought to be involved in silk production as well its rapid growth [6]. In *Aplysia*, the transcript of *Nsa2* homolog gene is found in the sensory neuron processes and is associated with synaptic plasticity [7]. However, the function of NSA2 in humans has not been reported thus far.

In our cell-based screening system integrating a promoter-Renilla luciferase reporter gene assay, fluorescence staining, automated microscopy and cellular phenotype assays to identify human novel genes associated with cell proliferation, we found the expression of *NSA2* could significantly up-regulate promoter-Renilla luciferase reporter plasmid (pRL) activity [8], it suggested that NSA2 might promote cell proliferation and we selected it to be characterized in more extensive experiments. In the present study, we constructed a panel of EGFP fusion proteins with different NSA2 regions and analyzed their intracellular distributions by confocal microscopy. We revealed the role of two nuclear localization signals (NLSs), also overlapped with nucleolar localization signals (NoLSs), in the nucleolar targeting of NSA2 for the first time. By investigating the effect of NSA2 in the cell cycle, our data suggests that *NSA2* may act as a cell cycle repressor and plays a role in cell proliferation.

Materials and methods

Cell lines and reagents. HeLa (human cervical carcinoma), HEK293T (human embryonic kidney) and A549 (human epithelial lung adenocarcinoma) cell lines were maintained in Dulbecco's modified Eagle's medium (Life Technologies, Carlsbad, CA, USA) supplemented with 10% FBS and 2 mM L-glutamine. The K562 (human erythroleukemic cells) and PC-3 (human prostate adenocarcinoma) cell lines were cultured in RMPI-1640 supplemented with 10% FBS and 2 mM L-glutamine. All cells were maintained at 37 °C in a humidified atmosphere with 5% CO_2. Anti-β-actin antibody and Hoechst stain were from Sigma–Aldrich (St. Louis, MO, USA). Anti-HSP90 antibody and anti-histone H3 antibody were purchased from Cell Signaling Technology (Danvers, MA, USA).

* Corresponding author. Address: Department of Immunology, School of Basic Medical Sciences, Peking University, No. 38 Xueyuan Road, Beijing 100191, PR China. Fax: +86 10 82801149.
E-mail address: hongshan@bjmu.edu.cn (H. Zhao).
[1] Both authors contributed equally to this study.

0006-291X/$ - see front matter © 2009 Elsevier Inc. All rights reserved.
doi:10.1016/j.bbrc.2009.11.114

IRDye™ 800-conjugated secondary antibodies against mouse and rabbit IgG, and IRDye™ 800-conjugated antibody against Green Fluorescent Protein (GFP) were purchased from LI-COR Bioscience (Lincoln, NE, USA). SiRNA against *NSA2* (sc-91967) was designed and purchased from Santa Cruz biotechnology, Inc. (Santa Cruz, CA, USA). Propidium iodide (PI) was obtained from the Beijing Biosea Biotechnology Co. (Beijing, China). The tissue cDNA library was purchased from Clonetech (Mountain View, CA, USA). Restriction endonuleases *Eco*RI, *Hin*dIII, and *Bam*HI were purchased from TaKaRa Biotechnology (Dalian) Co., Ltd. (Dalian, Liaoning, China). Protease inhibitor cocktail tablets were obtained from Roche Applied Science (Rotkreuz, Switzerland).

Polyclonal anti-NSA2 antibody preparation. Two peptides, RNTKQKNDEKTPQGAVC and DYHEKKRKKESREAHEC, which correspond to the two hydrophilic regions of the NSA2 protein, were synthesized and conjugated to keyhole limpet hemocyanin (KLH) by Chinese Peptide (Hangzhou, Zhejiang, China). Adult New Zealand white rabbits were immunized with a combination of the two tagged peptides at 6-week intervals, with immune serum collected 14 days after the immunizations. The serum was screened by indirect ELISA and antibodies purified by protein G and peptide affinity chromatography (data not shown). The resulting antibody was verified by Western blot and used in analysis of *NSA2* knockdown.

Constructs and transient transfections. Human *NSA2* cDNA was subcloned into the pcDNA3.1-Myc-His(−)B (pCDB) vector (Invitrogen, Carlsbad, CA, USA) without a C-terminal myc-tag, pEGFP-C3 vector and pEGFP-N1 vector (Clontech). A series of truncated NSA2 gene constructs were then subcloned into pEGFP-N1 vectors with a C-terminal GFP-tag. All constructs were confirmed by DNA sequencing.

293T cells were transfected by Lipofectamine 2000 (Invitrogen) according to the manufacturer's instruction. Transfections of HeLa, K562, PC-3 cells were performed by electroporation with a single pulse of 120 V, 20 ms, with 10 μg plasmid/10^6 cells in 2-mm gap cuvettes using an ECM 830 Square Wave Electroporation System (BTX, San Diego, CA, USA). Cells with more than 80% transfection efficiency were used for further experiments.

Immunofluorescence staining and microscopy. Cells were grown in glass-bottom microwell dishes (MatTek, Ashland, MA, USA) and transfected with the indicated vectors. After 24 h, the cells were incubated with corresponding antibodies, and then incubated with Hoechst stain (1:1000) for 5 min. Samples were observed using an Olympus Fluoview FV300 laser-scanning confocal microscopy (Olympus, Tokyo, Japan).

Extraction of cytoplasmic and nuclear proteins. HeLa cytoplasmic and nuclear proteins were extracted by using ProteoJET™ Cytoplasmic and Nuclear Protein Extraction Kit (Fermentas, Glen Burnie, MD, USA) according to the manufacturers' protocol.

RNA isolation, reverse transcriptase-polymerase chain reaction (RT-PCR) and quantitative real-time PCR analysis. RNA was extracted by using TRIzol reagent (Invitrogen), and reverse transcription (RT) was performed with ThermoSCRIPT RT-PCR System (Invitrogen) according to the manufacturer's protocol. PCR primers and conditions were as follows: forward primer, 5′-ATGCCACAGAATGAATA TATTGA-3′; reverse primer, 5′-AACCAGTAAGACTGCATTTATA-CATCC-3′; 25 amplification cycles (94 °C for 30 s, 52 °C for 30 s, 72 °C for 30 s). PCR products were separated on a 1.0% agarose gel and visualized by ethidium bromide staining. Real-time PCR analysis of NSA2 was performed with the following primers: forward primer, 5′-CTGCTGGACAGAGAGGGACAA-3′; reverse primer, 5′-TTTCTCCCTGGGCACGTACTT-3′. The annealing temperature for the real-time PCR was 60 °C for 45 cycles. GAPDH was amplified as an internal control.

Protein preparation and Western blot analysis. Cells were washed twice with ice-cold phosphate-buffered saline (PBS) and lysed in RIPA lysis buffer (50 mM Tris–HCl, pH 7.4; 150 mM NaCl; 1% deoxycholate Na; 1% NP-40; 0.1% sodium dodecylsulfate, with freshly added protease inhibitor cocktail) for 30 min at 4 °C. Cell lysates were clarified by centrifugation at 4 °C at 16000*g* for 20 min. Protein concentrations were determined using the BCA protein assay reagent (Pierce, USA). Equal amounts of protein were electrophoresed by SDS–PAGE and transferred onto a nitrocellulose membrane (Amersham Pharmacia, UK). Membranes were blocked in Tris-buffered saline containing 0.1% Tween-20 (TBST) and 5% nonfat milk and then incubated overnight at 4 °C with the appropriate primary antibody. After washing in TBST buffer, the membranes were incubated for 1 h with the corresponding IRDye™ 800-conjugated secondary antibody. The blots were scanned using an Odyssey Imaging System (LI-COR Bioscience).

Cell proliferation assay. Cell proliferation was evaluated using a CCK8 assay and cell counting. Transfected HEK293 cells (1000 cells/well) were seeded in 96-well plates and tested by using CCK8 (Cell Counting kit-8) kit according to the manufacturer's protocol. Briefly, 10 μl of CCK8 solution (Dojindo, Kumamoto, Japan) was added to each well, and the samples were incubated for the indicated times (2–4 h) before the absorbance was measured at 450 nm.

Transfected K562 cells (6×10^3/well) were seeded in 12-well plates. At the indicated time points, cells expressing different plasmids or siRNAs were trypsinized and counted by trypan blue exclusion using a Coulter counter (Vi-Cell™ XR Cell Viability Analyzer, Beckman, Fullerton, CA, USA). The results are presented as mean ± standard deviation (SD).

Cell cycle analysis. 293T cells were serum starved for 12 h and then plated in 6-wells (3×10^5cells/well). After 24 h, cells were transfected with plasmids or siRNAs. Transfected cells were fixed in 70% ethanol overnight at 4 °C. After washing with PBS, cells were incubated with Rnase A (0.5 mg/ml) (Sigma) at 37 °C for 30 min. Finally, the cells were stained with PI (50 μg/ml) and analyzed by fluorescence-activated cell sorter analysis (FACS) (BD, San Jose, CA, USA).

Results

Cloning and bioinformatic analysis of human NSA2

The full-length human *NSA2* cDNA clone (GenBank Accession No. NM_014886) was isolated from mixed tissue cDNA panels (Clontech, CA). The *NSA2* cDNA encodes a protein of 260 amino acids with a predicted molecular mass of 30 kDa and a theoretical isoelectric point of 10.28. The full-length cDNA sequence of *NSA2* and the amino acid sequence of the corresponding protein are shown in Fig. 1A. *NSA2* is located on chromosome 5q13.3, and encompasses 6 exons and 5 introns that span nearly 4596 kb (Fig. 1B). The NSA2 gene is highly conserved among vertebrates (Fig. 1C); it shares 100% identity with the canis family and pan troglodytes, and 62.1% identity with the yeast ortholog Nsa2. Analysis of the NSA2 amino acid sequence by Simple Modular Architecture Research Tool (smart.embl-heidelberg.de) revealed a conserved functional domain Ribosomal_S8e from 1 to 237 amino acids, named after the Rps8 eukaryotic and archebacterial ribosomal protein [9].

Expression profiles of NSA2

The expression patterns of the *NSA2* gene in various human tissues and cell lines were analyzed by RT-PCR and Western blot. The NSA2 transcripts were detected in normal human tissues (Fig. 2A), 10 non-leukemia cancer cell lines (Fig. 2B) and 9 leukemia cell lines (Fig. 2C). *NSA2* mRNA was up-regulated in cells stimulated by TGF-β (Fig. 2D). The specificity of the anti-NSA2 antibody was tested

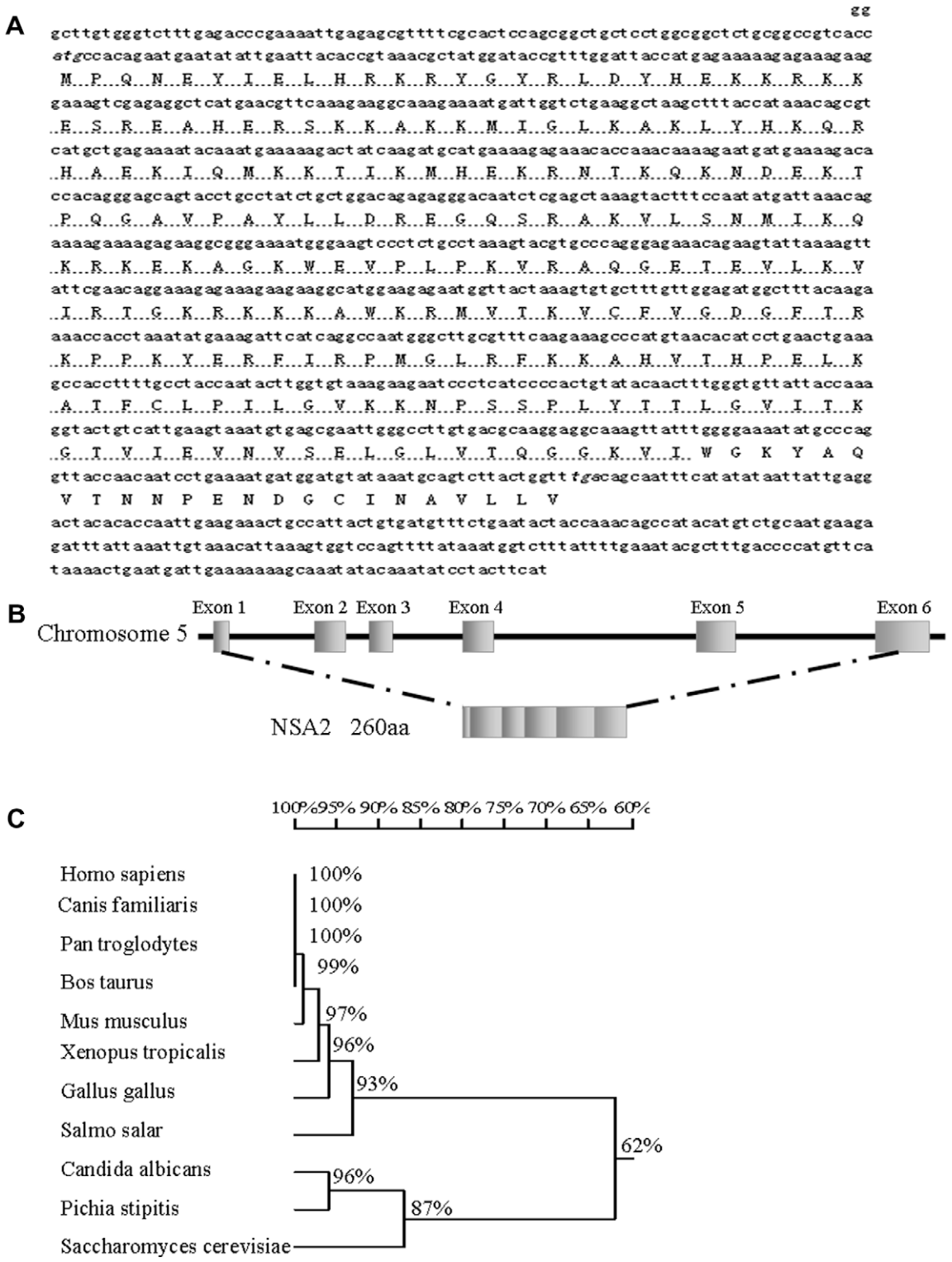

Fig. 1. Identification and sequence analysis of *NSA2*. (A) cDNA and amino acid sequences of human *NSA2*. The start and stop codons are italicized. The Ribosomal_S8e domain is indicated with a broken line. (B) The schematic map of the *NSA2* gene and cDNA structure. The boxes show the exons with their relative sizes and the positions in the *NSA2* gene. (C) Phylogenetic analysis of *NSA2*.

against the over-expressed EGFP-NSA2 in HeLa cells in a Western blot (Fig. 2E). A band of ~30 kDa could be detected, which was consistent with the calculated molecular weight of the NSA2 protein. By using this antibody, protein expression of the endogenous NSA2 was detected in various human cancer cell lines (Fig. 2F). These results suggest that the NSA2 protein is ubiquitously expressed in high levels.

Mapping the nucleolar localization signals of NSA2

As shown in Fig. 3A, the NSA2 protein was specifically expressed in the nuclear region of HeLa cells. We fused the *NSA2* cDNA to the 3-end of the *GFP* cDNA in the pEGFP-C3 vector and to the 5-end of the *GFP* cDNA in the pEGFP-N1 vector. NSA2-GFP expressed in HeLa cells was observed in the nucleolus and

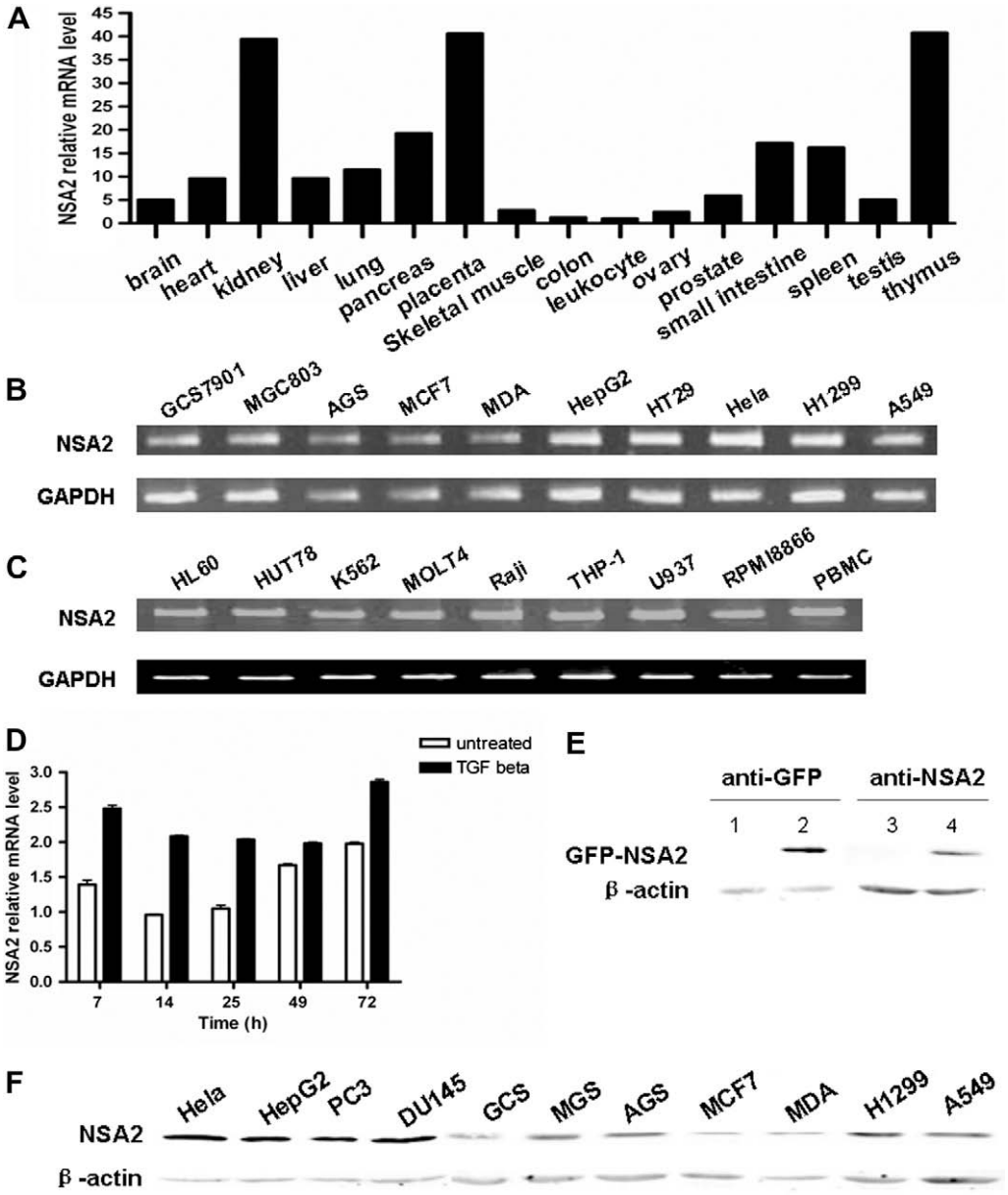

Fig. 2. Expression profiles of *NSA2*. Real-time PCR analysis shows the mRNA expression of *NSA2* in human normal tissues (A) and A549 cells stimulated with or without TGF-β (5 ng/ml) at the indicated time (B). The data are represented as mean ± SD. NSA2 mRNA expression was also analyzed by RT-PCR in human cancer cell lines (C) and human leukemia cell lines (D). GAPDH was used as an internal control. (E) HeLa cells were transfected with pEGFP-C3 vector or pEGFP-NSA2 vector. The proteins were extracted 48 h later and detected with anti-NSA2 antibody and anti-GFP antibody as a positive control. (F) Expression levels of endogenous NSA2 in multiple human cell lines were analyzed by Western blot. β-Actin expression was detected as an internal control.

co-localized with nucleolin (Fig. 3B). The subcellar distribution of GFP-NSA2 was identical.

The sequence analysis predicts two putative NLS spanning amino acids 1–52 (NLS1) and 131–154 (NLS2), as depicted schematically in Fig. 3C. To analyze the role of the suggested NLS sequences of *NSA2* in targeting to the nucleolus, a series of constructs carrying various deletions of NSA2 sequences were fused to the N1-pEGFP plasmid (Fig. 3D). These constructs were transfected into HeLa cells and the fluorescent fusion proteins were monitored under a confocal microscope. As shown in Fig. 2E, the pEGFP-N1 was expressed in both the nucleus and cytoplasm. In contrast, all of the I-EGFP, II-EGFP, and III-EGFP fusion proteins, which contained the NLS1, NLS2, and the intermediate sequences (aa 53–130), respectively, exhibited diffuse nuclear staining and clear nucleolar staining. Expression of the C-terminal region of NSA2 (aa 155–266) (IV-EGFP) displayed nuclear and cytoplasmic diffusion staining, similar to the results with the pEGFP-N1 vector.

We also constructed various deletion mutants. An EGFP protein fused to the NSA2 region deleted of NLS2 (Fig. 3E, V) consistently showed nucleolar staining. The same pattern was also seen when the cells were transfected with the *NSA2* region in deleted of NLS1 (Fig. 3E, VI) or of both NLS1 and NLS2 (Fig. 3E, VII). The NLS1 comprises two bipartite NLSs (^{10}HRKRYGYRLDYHEKKRKK^{27} and ^{23}KKRKKESREAHERSKKAKKM^{42}), and both of these appeared to be responsible for nuclear staining and nucleolar accumulation (Fig. 3E, VIII and IX). However, flanking both sides of the NLS1 region with the two bipartite NLSs deleted displayed cytoplasmic and nuclear diffuse staining, resembling the localization of EGFP alone (Fig. 3C, X).

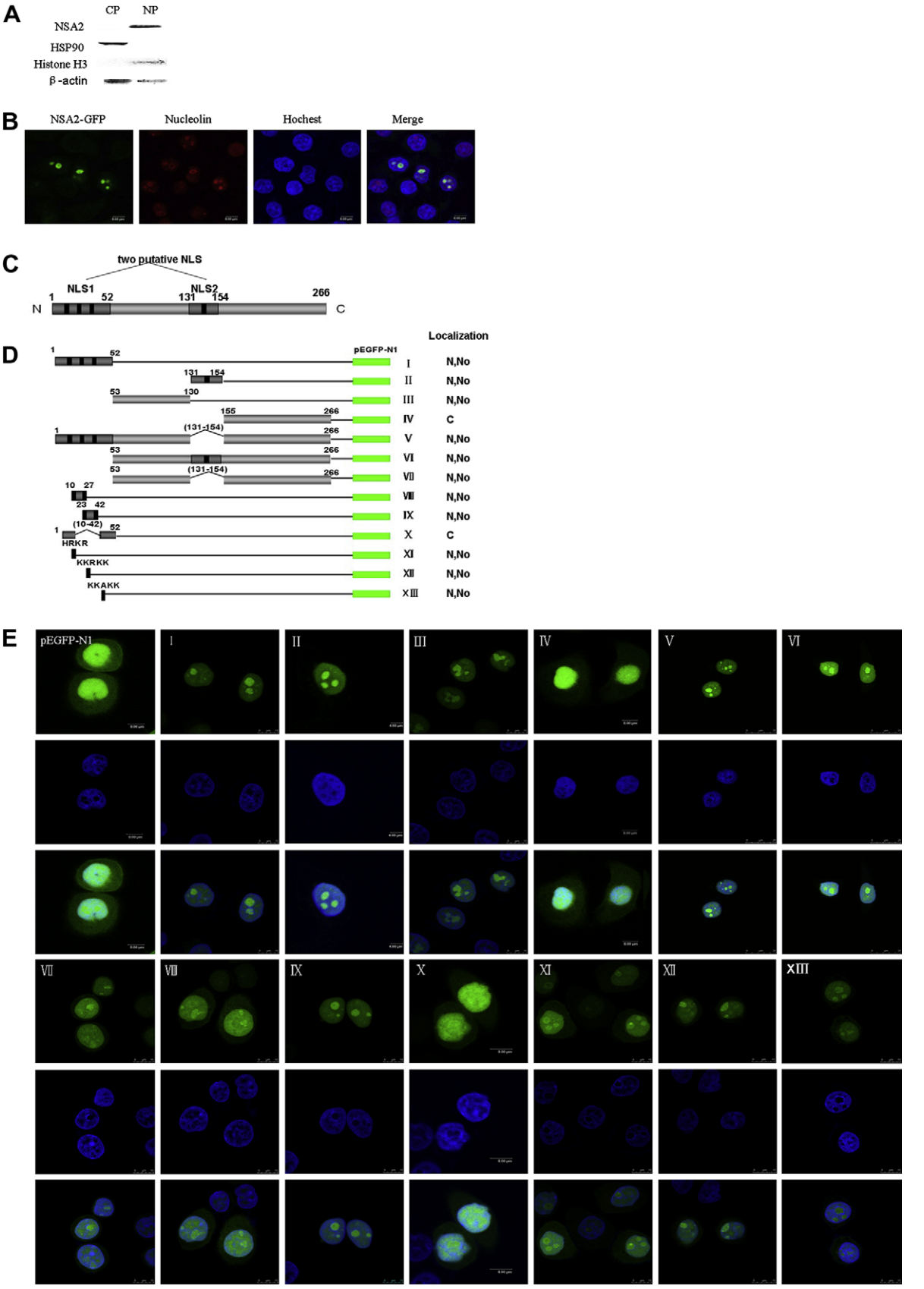

Fig. 3. NLS regions of NSA2. (A) NSA2 protein was detected in the nuclear extracting proteins (NP) of HeLa cells, but not in the cytoplasmic extracting proteins (CP). (B) EGFP-NSA2 co-localized with nucleolin in HeLa cells. (C) Full-length NSA2 with two putative NLSs. (D) Constructs with deleted sequences within NSA2 fused with EGFP are shown schematically. (E) The subcellular localization of these constructs and EGFP alone in HeLa cells. N, nuclear; No, nucleolus; C, both nuclear and cytoplasmic diffuse staining.

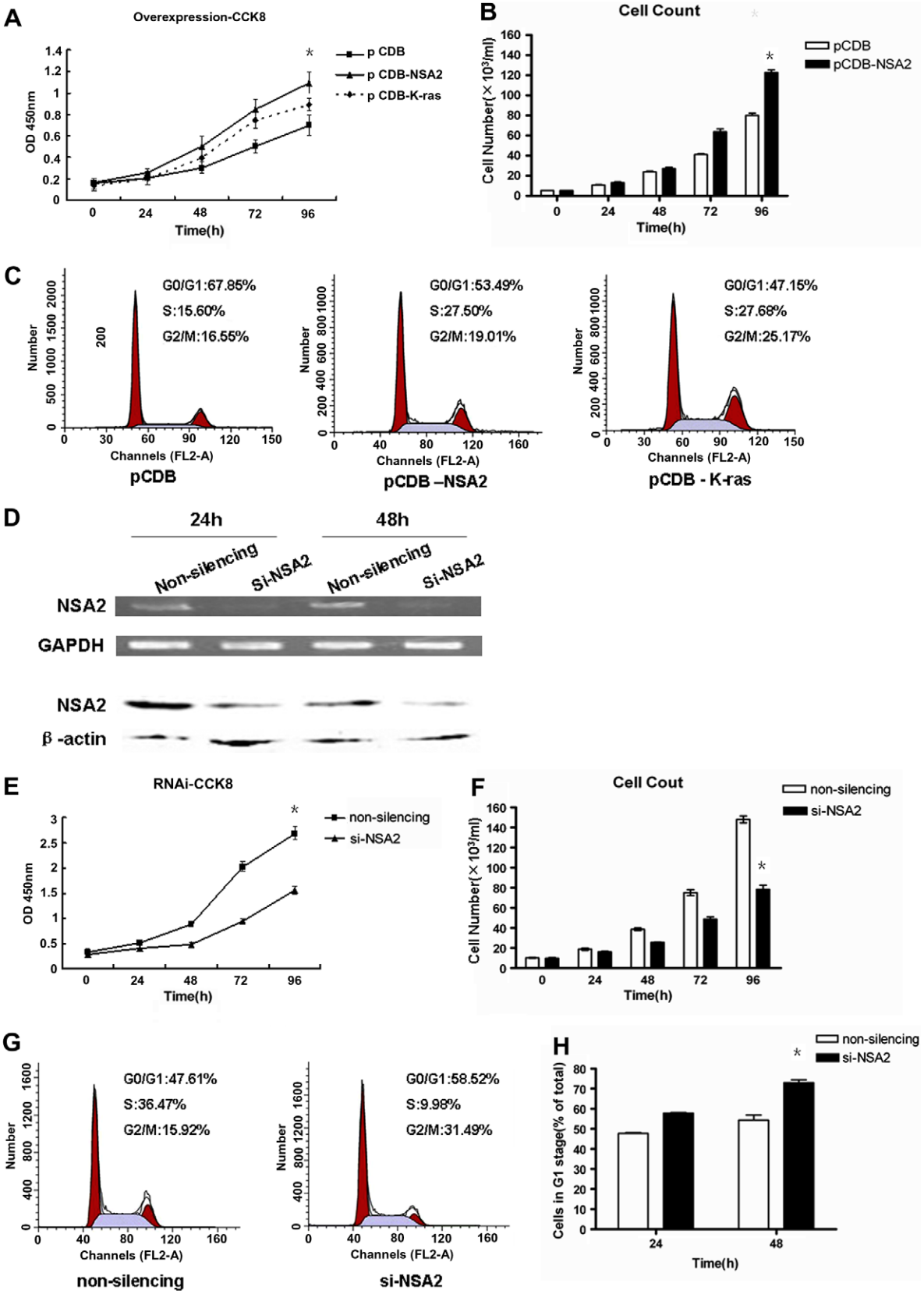

Fig. 4. Function of NSA2 in cell proliferation and cell cycle. (A) CCK8 assay for PC-3 cells transfected with pCDB (vector control), pCDB-NSA2, or pCDB-K-ras (positive control). Cells were collected at indicated times, processed and then the absorbance was measured at 450 nm. (B) Growth curve of K562 cells transiently transfected with pCDB, pCDB-NSA2, and pCDB-K-ras. Cells were collected at the indicated times and counted on a Coulter cell counter. (C) A representative FACS profile of cells transfected with pCDB, pCDB-NSA2, or pCDB-K-ras. Cells were collected 24 h after transfection and analyzed by flow cytometry. Data are representative of three separate experiments. (D) siRNA against *NSA2* inhibited *NSA2* expression at both mRNA and protein levels. (E) CCK8 assay for NSA2 knockdown by double-stranded siRNAs in PC3 cells. (F) Growth curve of K562 cells transiently transfected with siNSA2 and non-silencing siRNA. Cell proliferation was measured using a Coulter counter. (G) A representative FACS profile of cells transfected with siNSA2 and non-silencing siRNA. Cells were collected 24 h after transfection and analyzed by flow cytometry. (H) Graphic representation of the percentage of cells in G1 phase. Transfected cells were collected after 24 h and 48 h. $^{*}P < 0.05$, compared with mock-transfected cells. Error bars represent SEM.

Basic amino acid residues have been speculated to be important in nucleolus targeting. The NLS1 contains three clusters of basic residues at positions 10–13, 23–28, and 37–41 with sequences of HRKR, KKRKK, and KKAKK, respectively. All three clusters can lead to nucleolar accumulation (Fig. 3C, XI–XIII). While it is possible that the nucleolar accumulations of GFP-NSA2 and its variants were artifacts of high expression levels, we also examined their localization patterns as early as 12 h after transfection when expression levels were low, and the results were the same.

Over-expression of NSA2 promotes cell proliferation and G1/S transition in the cell cycle

PC-3 cells were transiently transfected with NSA2 expression vectors followed by CCK8 measurement of cell proliferation. As shown in Fig. 4A, an increase in cell proliferation was noted, during a 5-d period, in cells transfected with NSA2 compared with mock-transfected cells. Over-expression of NSA2 in K562 also resulted in a remarkable increase in the cell number as determined by using a Coulter cell counter (Fig. 4B). We obtained similar results from the experiments in 293T and HeLa cells.

To explore the possible roles of NSA2 in controlling cell cycle, we examined the cell cycles of transfected cells by FACS (Fig. 4C). The results showed that at 24 h after transfection, over-expression of NSA2 resulted in a 14.36% decrease of G1 phase cells and an 11.90% increase of S-phase cells compared with the vector control group. These results suggest that NSA2 plays a role in the protein synthesis and DNA synthesis in different cells.

Down-regulation of NSA2 inhibits cell proliferation and G1/S transition in the cell cycle

Since over-expression of NSA2 promoted cell proliferation and G1/S transition, we examined the effect of down-regulating NSA2 on these parameters. SiRNA against *NSA2* was used to reduce its expression in PC3 cells. Non-silencing siRNA or siNSA2 was transfected into PC3 cells. At 24 and 48 h after transfection, both *NSA2* mRNA and NSA2 protein levels were significantly decreased in cells that were transfected with siNSA2, as assessed by RT-PCR and Western blot (Fig. 4D).

As shown in Fig. 4E, siNSA2 resulted in a decrease in PC-3 cell proliferation compared with the control. Similar results were also obtained in K562 cells by cell counting (Fig. 4F). The inhibition of G1/S transition was observed in cells transfected with siRNA against NSA2, but not in cells transfected with non-silencing siRNA (Fig. 4G). Furthermore, siNSA2-transfected cells consistently exhibited a higher percentage of cells in G1 phase of the cell cycle (Fig. 4H).

Discussion

In this study, we report that human NSA2 is located in the nucleolus of cells and contains multiple nucleolar localization signals (NoLSs). The nucleolus is the most prominent structure in a cell nucleus and defined as a genetically determined element. The functional annotation of proteins in the human nucleolus has been drafted [10], while a large fraction of the uncharacterized proteins confer a role in ribosome biogenesis complexes. There are also nucleolar protein complexes involved in DNA repair, tRNA processing, DNA replication, and transcription initiation. Emerging evidence also describes other unconventional roles for the nucleolus, such as in stress sensing and the control of cellular activity [11,12].

Several NoLSs have been identified by previous studies [13–16], but sequence analysis of nucleolar proteins did not lead to the identification of a general NoLS [13–15]. An important characteristic of the nucleolar localization sequences is that they overlap with nuclear localization signals (NLSs) [13,14,16]. NLSs are often characterized by clusters of positively charged amino acids such as lysine (K), arginine (R), or histidine (H) [17]. Except NSA2, other proteins such as parafibromin, MDM2 and $p14^{ARF}$ have also been found to contain NoLSs composed of clusters of basic amino acids highly similar to or overlapping those identified in NLSs [18–20]. The nucleolar localization of proteins possibly relies on direct or indirect interaction with the ribosomal DNA, RNA, or protein [21].

In this study, we identified two NLSs in NSA2 for the first time. There are three clusters of NLS1 which play roles in the nuclear localization, and all of them can function independently. However, unlike the classical bipartite NLS consisting of a defined spacer of 8–10 non-basic amino acids between two clusters of basic amino acids, the NLS1 of NSA2 is composed of three clusters of basic amino acids or two overlapping bipartite NLSs. Interestingly, both the mutant NSA2 lacking NLSs and the intermediate sequences between the two NLSs still localized to the nucleolus, suggesting the existence of at least one additional NoLS between NLS1 and NLS2 of NSA2. This intermediate region may also modulate NSA2 localization by binding to protein or nucleic acid constituents of the nucleoli.

Nucleolar proteins are increasingly recognized as possible regulators of cell growth [22,23]. Besides, nucleolar breakdown and division are closely coordinated with mitosis and regulation of the cell cycle [24]. We demonstrated that over-expression of NSA2 could promote the proliferation of different cell lines and facilitate G1 to S transition in the cell cycle, while down-regulation of NSA2 by siRNA showed the opposite effect. Therefore, we can conclude that NSA2 is crucial for cell growth since the apparent proliferation arrest corresponded to an increase in the G1 phase cell population and a decrease in the number of cells in the S and G2 phase. However, the mechanisms used by NSA2 to affect the cell cycle are still unknown.

Bioinformatics analysis shows that NSA2 contains the conserved Ribosomal_S8e domain and implies that NSA2 belongs to the ribosomal protein superfamily. The nucleolus has been determined to be the site of ribosomal RNA (rRNA) transcription, pre-rRNA processing and ribosome subunit assembly [25]. Cell proliferation depends on protein synthesis through ribosome biogenesis [26,27]. For example, it was shown that down-regulation of ribosomal protein L15 expression inhibited SGC7901 cell growth [28]. Furthermore, the yeast homolog Nsa2 was demonstrated to be a pre-ribosomal factor required for adequate processing of the ITS2, which separates 25S and 5.8S rRNA. The expression of *NSA2* was able to restore growth in a *Nsa2*-deleted strain [5]. Therefore, we inferred that NSA2 may have similar activities to that of Nsa2 and appears to have essential roles in ribosomal biogenesis as well as regulation of cell proliferation.

In conclusion, our experimental data indicate that NSA2 is a novel nucleolus protein which has multiple nucleolar localization signals. Over-expression of NSA2 induced cell proliferation and G1/S cell cycle transition. Suppression of NSA2 by small interfering RNA (siRNA) inhibited the G1/S transition in cell cycle and cell proliferation. Therefore, NSA2 plays an important role in cell growth and cell cycle regulation, the mechanism of which will require further study.

Acknowledgments

This work was supported by grants from the National High Technology Research and Development Program of China (2006AA02A305) and the National Key New Drug Creation Program of China (2009ZX09503-004).

References

[1] X. Wu, G. Ivanova, M. Merup, M. Jansson, B. Stellan, D. Grander, E. Zabarovsky, G. Gahrton, S. Einhorn, Molecular analysis of the human chromosome 5q13.3 region in patients with hairy cell leukemia and identification of tumor suppressor gene candidates, Genomics 60 (1999) 161–171.

[2] F. Stanchi, E. Bertocco, S. Toppo, R. Dioguardi, B. Simionati, N. Cannata, R. Zimbello, G. Lanfranchi, G. Valle, Characterization of 16 novel human genes showing high similarity to yeast sequences, Yeast 18 (2001) 69–80.

[3] A. Scherl, Y. Coute, C. Deon, A. Calle, K. Kindbeiter, J.C. Sanchez, A. Greco, D. Hochstrasser, J.J. Diaz, Functional proteomic analysis of human nucleolus, Mol. Biol. Cell 13 (2002) 4100–4109.

[4] J.S. Andersen, Y.W. Lam, A.K. Leung, S.E. Ong, C.E. Lyon, A.I. Lamond, M. Mann, Nucleolar proteome dynamics, Nature 433 (2005) 77–83.

[5] A. Lebreton, C. Saveanu, L. Decourty, A. Jacquier, M. Fromont-Racine, Nsa2 is an unstable, conserved factor required for the maturation of 27 SB pre-rRNAs, J. Biol. Chem. 281 (2006) 27099–27108.

[6] J.L. Wang, Y.P. Zhang, Y.Y. Gu, J.X. Wang, X.F. Zhao, Function of a TGF-beta inducible nuclear protein in the silk gland in *Bombyx mori*, Insect. Mol. Biol. 18 (2009) 243–251.

[7] L.L. Moroz, J.R. Edwards, S.V. Puthanveettil, A.B. Kohn, T. Ha, A. Heyland, B. Knudsen, A. Sahni, F. Yu, L. Liu, S. Jezzini, P. Lovell, W. Iannucculli, M. Chen, T. Nguyen, H. Sheng, R. Shaw, S. Kalachikov, Y.V. Panchin, W. Farmerie, J.J. Russo, J. Ju, E.R. Kandel, Neuronal transcriptome of aplysia: neuronal compartments and circuitry, Cell 127 (2006) 1453–1467.

[8] X. Ma, X. Wang, X. Gao, L. Wang, Y. Lu, P. Gao, W. Deng, P. Yu, J. Ma, J. Guo, H. Cheng, C. Zhang, T. Shi, D. Ma, Identification of five human novel genes associated with cell proliferation by cell-based screening from an expressed cDNA ORF library, Life Sci. 81 (2007) 1141–1151.

[9] I. Letunic, L. Goodstadt, N.J. Dickens, T. Doerks, J. Schultz, R. Mott, F. Ciccarelli, R.R. Copley, C.P. Ponting, P. Bork, Recent improvements to the SMART domain-based sequence annotation resource, Nucleic Acids Res. 30 (2002) 242–244.

[10] A.M. Hinsby, L. Kiemer, E.O. Karlberg, K. Lage, A. Fausboll, A.S. Juncker, J.S. Andersen, M. Mann, S. Brunak, A wiring of the human nucleolus, Mol. Cell 22 (2006) 285–295.

[11] C. Mayer, H. Bierhoff, I. Grummt, The nucleolus as a stress sensor: JNK2 inactivates the transcription factor TIF-IA and down-regulates rRNA synthesis, Genes Dev. 19 (2005) 933–941.

[12] M.O. Olson, Sensing cellular stress: another new function for the nucleolus?, Sci STKE 2004 (2004) 10.

[13] A.C. Timmers, R. Stuger, P.J. Schaap, J. van 't Riet, H.A. Raue, Nuclear and nucleolar localization of *Saccharomyces cerevisiae* ribosomal proteins S22 and S25, FEBS Lett. 452 (1999) 335–340.

[14] R.R. Rowland, D. Yoo, Nucleolar-cytoplasmic shuttling of PRRSV nucleocapsid protein: a simple case of molecular mimicry or the complex regulation by nuclear import Nucleolar localization and nuclear export signal sequences., Virus Res. 95 (2003) 23–33.

[15] F. Catez, M. Erard, N. Schaerer-Uthurralt, K. Kindbeiter, J.J. Madjar, J.J. Diaz, Unique motif for nucleolar retention and nuclear export regulated by phosphorylation, Mol. Cell. Biol. 22 (2002) 1126–1139.

[16] Z. Sheng, J.A. Lewis, W.J. Chirico, Nuclear and nucleolar localization of 18-kDa fibroblast growth factor-2 is controlled by C-terminal signals, J. Biol. Chem. 279 (2004) 40153–40160.

[17] C. Dingwall, R.A. Laskey, Nuclear targeting sequences—a consensus?, Trends Biochem Sci. 16 (1991) 478–481.

[18] M.A. Hahn, D.J. Marsh, Nucleolar localization of parafibromin is mediated by three nucleolar localization signals, FEBS Lett. 581 (2007) 5070–5074.

[19] M.A. Lohrum, M. Ashcroft, M.H. Kubbutat, K.H. Vousden, Identification of a cryptic nucleolar-localization signal in MDM2, Nat. Cell Biol. 2 (2000) 179–181.

[20] J.D. Weber, M.L. Kuo, B. Bothner, E.L. DiGiammarino, R.W. Kriwacki, M.F. Roussel, C.J. Sherr, Cooperative signals governing ARF-mdm2 interaction and nucleolar localization of the complex, Mol. Cell. Biol. 20 (2000) 2517–2528.

[21] M. Carmo-Fonseca, L. Mendes-Soares, I. Campos, To be or not to be in the nucleolus, Nat. Cell Biol. 2 (2000) E107–E112.

[22] L. Comai, The nucleolus: a paradigm for cell proliferation and aging, Braz. J. Med. Biol. Res. 32 (1999) 1473–1478.

[23] Y.C. Du, B. Stillman, Yph1p an ORC-interacting protein: potential links between cell proliferation control, DNA replication, and ribosome biogenesis, Cell 109 (2002) 835–848.

[24] M.O. Olson, M. Dundr, The moving parts of the nucleolus, Histochem. Cell Biol. 123 (2005) 203–216.

[25] M.O. Olson, K. Hingorani, A. Szebeni, Conventional and nonconventional roles of the nucleolus, Int. Rev. Cytol. 219 (2002) 199–266.

[26] H. Lempiainen, D. Shore, Growth control and ribosome biogenesis, Curr. Opin. Cell Biol. (2009).

[27] C. Mayer, I. Grummt, Ribosome biogenesis and cell growth: mTOR coordinates transcription by all three classes of nuclear RNA polymerases, Oncogene 25 (2006) 6384–6391.

[28] H. Wang, L.N. Zhao, K.Z. Li, R. Ling, X.J. Li, L. Wang, Overexpression of ribosomal protein L15 is associated with cell proliferation in gastric cancer, BMC Cancer 6 (2006) 91.